Solid Earth Discuss., 6, 511–534, 2014
www.solid-earth-discuss.net/6/511/2014/
doi:10.5194/sed-6-511-2014

Solid Earth
Discussions
Open Access

Velocity structure and the role of fluids in the West Bohemia Seismic Zone

C. Alexandrakis[1], **M. Calò**[2], **F. Bouchaala**[3], **and V. Vavryčuk**[4]

[1]Institute of Geophysics and Geoinformatics, TU Bergakademie Freiberg, Freiberg, Germany
[2]Berkeley Seismological Laboratory, Berkeley, USA
[3]The Petroleum Institute, Abu Dhabi, United Arab Emirates
[4]Institute of Geophysics, Academy of Sciences, Prague, Czech Republic

Received: 27 January 2014 – Accepted: 29 January 2014 – Published: 11 February 2014

Correspondence to: C. Alexandrakis (catherine.alexandrakis@geophysik.tu-freiberg.de)

Published by Copernicus Publications on behalf of the European Geosciences Union.

Title Page
Abstract Introduction
Conclusions References
Tables Figures
I◀ ▶I
◀ ▶
Back Close
Full Screen / Esc
Printer-friendly Version
Interactive Discussion

Abstract

In this study, we apply the double-difference tomography method to investigate the detailed 3-D structure within and around the Nový Kostel seismic zone, an area in the Czech Republic known for frequent occurrences of earthquake swarms. We use data from the extensively analyzed 2008 swarm, which has known focal mechanisms, principal faults, tectonic stress, source migration and other basic characteristics. We selected about 500 microearthquakes recorded at 22 local seismic stations of the West Bohemia Network (WEBNET). Applying double-difference tomography, combined with Weighted Average Model post-processing to correct for parameter dependence effects, we produce and interpret 3-D models of the Vp-to-Vs ratio (Vp/Vs) in and around the focal zone. The modeled Vp-to-Vs ratio shows several distinct structures, namely an area of high Vp-to-Vs ratio correlating with the microearthquakes, and a layer of low values directly above it. These structures may reflect changes in lithology and/or fluid concentration. The overlaying low Vp-to-Vs ratio layer coincides with high density metamorphic unit associated with the Fichtelgebirge (Smrčiny) granitic intrusion. It is possible that the base of the layer acts as a fluid trap, resulting in the observed periodic swarms.

1 Introduction

The Nový Kostel seismic zone is the most seismically active area in West Bohemia, Czech Republic, a region known for frequent earthquake swarms (Fig. 1). Isotope analysis (mainly He3/He4) indicates that the fluids released from gas vents and springs within and around the Cheb Basin are magmatic in nature (Bräuer et al., 2005; Weise et al., 2001). This has led to the hypothesis that migrating fluids play a major role in the swarm activity (Bräuer et al., 2005; Geissler et al., 2005; Hainzl et al., 2012; Špičák and Horálek 2001).

Seismic swarms in the Nový Kostel area occur at the junction of the Mariánské-Lázně Fault and the Počátky-Plesná Fault Zone (Bankwitz et al., 2003; Peterek et al., 2011). The 2008 swarm had two dominant focal mechanisms with principal fault planes oriented at 169° and 304° (Vavryčuk, 2011). The 169° principal fault corresponds well with the Počátky-Plesná Fault segments in the Nový Kostel Zone (Bankwitz et al., 2003) and the 304° principal fault is approximately parallel to the Gera-Jáchymov Fault Zone (Švancara et al., 2008).

Several studies have produced models of the crustal structure using a variety of geophysical methods and data (e.g. Hrubcová et al., 2005, 2013; Málek et al., 2001; Mlčoch and Skácelová 2009; Růžek et al., 2007; Tomek et al., 1997). Many of these studies were aimed at investigating the deep crust and therefore did not resolve the focal zone structures. In this study, double-difference tomography is used to investigate the velocity structure in the focal zone. It is able to image small-scale velocity heterogeneities near a focal zone which contains numerous, closely-spaced earthquakes recorded at seismic stations with good azimuthal coverage (Zhang and Thurber, 2003). These conditions are met by the clustered nature of the swarm and the West Bohemia network (WEBNET).

As with other seismic tomography methods, the starting model and inversion parameters may lead to artifacts (Kissling et al., 1994). Checkerboard and other synthetic tests are often used to determine the model resolution. However, it is difficult to deduce which features are artifacts of the parameterization. To address this problem, the Weighted Average Model (WAM) method is applied to the 2008 swarm data set (Calò et al., 2011). In this method, a suite of tomography models are calculated using a variety of reasonable input parameters. These models are averaged together, using an experimentally defined weighting factor. This process reduces bias and artifacts introduced by the a priori parametrization. Finally, extensive synthetic and resolution tests are used to confirm if the imaged velocity perturbations are resolved structures or artifacts.

Analysis of the model focuses on the rupture zone and the area directly above it. Structures observed in the Vp-to-Vs ratio (Vp/Vs) model are assessed in terms of local geology and the potential role of fluids in the swarm cycle.

2 Data

In this study, we use earthquakes that occurred during the 2008 Nový Kostel earthquake swarm (Fischer et al., 2010). It was one of the strongest recent swarms in the area. About 25 000 earthquakes with local magnitude greater than −0.5 were recorded by 23 WEBNET seismic stations (Fig. 1) and located using the program FASTHYPO (Herrmann, 1979). The epicenters form an elongated cluster (~ 4 km long) and hypocenters ranged between 7 and 11 km depth (Fischer et al., 2010). Bouchaala et al. (2013) used *P* wave and *S* wave arrival times and waveform cross-correlated times to relocate 483 selected events using HypoDD, a double-difference hypocenter location program (Waldhauser and Ellsworth, 2000). From these events, 473 are used in the *P* and *S*-velocity model tomography inversion. Over 8500 *P* wave and *S* wave arrivals were manually picked, resulting in 73 028 *P* wave and 72 967 *S* wave differential times and 63 656 *P* wave and 59 069 *S* wave cross-correlated times.

3 Methodology

3.1 Double-difference tomography

Double-difference tomography is an adaptation of local earthquake tomography (LET). Typically, LET is used to characterize structures between the source locations and the receivers. This method is most effective when the events are widely spread. Double-difference tomography is ideal for regions where the events are clustered closely together and can image the velocity structures immediately surrounding the cluster (Zhang and Thurber, 2003). This method is termed a “double-difference” tomography because the algorithm minimizes the modeled and observed traveltime difference between two earthquakes recorded at a single station. As a consequence, any influence from velocity anomalies or heterogeneities near the stations is removed due to the converging raypaths. Detailed knowledge of the near-surface geology is not required, but no shallow structures are determined. We use the program TomoDD (Zhang and Thurber, 2003) to jointly invert both P- and S-velocity models and hypocenter parameters. The P and S travel time catalogs are of comparable quality, size and raypath coverage, allowing for the determination of the P to S velocity ratio (Vp/Vs) calculated by direct division of the P- and S-velocity models.

The basic model for this study is the regional gradient P-velocity model of Málek et al. (2001) with a uniform Vp/Vs of 1.70. In the shallow part of the model (down to 4 km), layer thicknesses vary in order to maintain the velocity gradient. Below 4 km the model is defined in 1 km thick layers. The surface datum coincides with station NKC's elevation (609.94 m above sea level) and is centered at the swarm centroid (50.2105° N and 12.4508° E).

To reduce bias from the starting earthquake locations, both the FASTHYPO- and the HypoDD-located datasets are used in the WAM calculation.

3.2 Weighted average model analysis

As with many tomography algorithms, artifacts and model bias associated with the starting parametrization are difficult to quantify. The Weighted Average Model (WAM) method reduces the influence of the starting parametrization (Calò et al., 2011). In order to apply the WAM method, the basic seismic velocity model is defined on a 3-dimensional Cartesian grid. The model parametrization was then perturbed by shifting the nodes, changing node spacing and rotating the grid. Slightly faster and slower P-velocity models were also used by shifting the velocities in depth by ±300 m. In total, 12 unique starting velocity model parameterizations were defined and applied to the FASTHYPO and HypoDD-located datasets. The resulting 24 models were then used in the WAM calculation We also calculated the Weighted Standard Deviation (WSTD) for both the *P*- and *S*-velocity WAMs. The WSTD can indicate the stability of structures within the model. A high WSTD indicates that the velocity calculated at that location depends on the starting parametrization and is therefore an artifact.

4 Model resolution and synthetic tests

A first analysis of the velocity models and WAM showed a region with anomalously high *P*-velocities to the east of the focal zone, which also corresponds to an area of high WSTD (Fig. 2a). This region correlates to the raypath volume between the hypocenters and a single station. Synthetic tests confirmed that local changes in the surface geology would not produce such an anomaly (Fig. S1). To test if the anomaly was indeed related to the single station, the WAM analysis was repeated with the data from this station removed, resulting in reduced WSTD (Fig. 2b). When other stations were removed, the resulting models all contained the same high WSTD region as the WAM calculated with all of the stations included. Based on these tests, the raw data from this station was investigated and an error in the rupture onset time was found (A. Boušková, personal communication, 2013). Therefore, data from this station is excluded from the remaining tests and interpretations.

In order to further assess the model resolution, a series of synthetic and resolution tests were conducted. The first test assesses the dependence of the calculated models on the starting velocity model. This was accomplished by running the tomography with four perturbations of the starting model. The first two models were uniformly 0.5 $\mathrm{km\,s^{-1}}$ faster or slower than the regional model (Fig. S2). The Vp/Vs was not changed (ie. Vp/Vs = 1.7). In the last two models, the regional model's *P*-velocity was unchanged, but the Vp/Vs ratio was increased or decreased by 0.05 (Fig. S2). The resulting models show that the calculated *P*-velocity is influenced by the starting model. However, the Vp/Vs models all show similar structures and values, regardless of starting model (Fig. S2). This indicates that the resultant Vp/Vs model is stable and independent of the starting model.

The next set of tests investigates whether isolated velocity perturbations are recovered. This test is motivated by strong velocity and Vp/Vs perturbations observed along the fault plane and directly above the focal zone (see Sect. 5 for details). In the first four models (Fig. 3), a block mimicking the fault plane is perturbed. This block is 3 km wide in the x-direction, 6 km wide in the y-direction, 5 km deep and all earthquakes lie in this block. Two models have the P-velocities within the block perturbed by ±5 % (Vp/Vs = 1.7) (Fig. 3a and b). In the next two models, the Vp/Vs ratio is perturbed by 5 % within the block (Fig. 3c and d). All velocities and ratios outside the block correspond to the regional model of Málek et al. (2001). P and S synthetic traveltimes are calculated for the synthetic models using the WEBNET earthquake locations. In these tests, the synthetic data are limited to P and S catalog times and do not include a cross-correlation catalog. Therefore, these tests represent a "worst case" result.

The first four models (Fig. 3) show very good recovery in both shape and magnitude for the Vp/Vs ratios. The models with only P-velocity perturbation have well-restored P-velocities and Vp/Vs models. However, for the models with Vp/Vs perturbations, it is evident that the recovered P-velocities are strongly influenced. This indicates that areas corresponding to high or low P-velocity and Vp/Vs, the anomalous P-velocities are most likely artifacts. However, the Vp/Vs ratio is properly resolved and can be considered robust.

In the next four models, we add a 2 km thick contrasting layer above the blocks (Fig. S3). For example, in the model with high P-velocity along the fault plane, the velocities in the overlaying 2 km are decreased by 5 % (Fig. S3a), and in the model with the low Vp/Vs ratio block, the overlaying 2 km have a 5 % higher Vp/Vs ratio (Fig. S3c). As above, P and S synthetic traveltimes for each of the eight synthetic models are calculated using the WEBNET earthquake locations and no cross-correlated times are used.

As with the previous test, the recovered models show that the P-velocities are influenced by the Vp/Vs ratio (Fig. S3b and d). The influence of P-velocity changes on the Vp/Vs ratio is minor. These tests show that structures observed in the P-velocity model may be linked to changes in the Vp/Vs ratio. The calculated Vp/Vs models are more reliable and can be interpreted without consideration of *P*-velocity perturbations.

As a final test, we conduct a classical checkerboard for each model perturbation used in the WAM, and then calculate a checkerboard WAM. The regional model is used to create a checkerboard model with the *P*-velocities alternating ±5 % within the layers. The Vp/Vs is kept constant at 1.7. Cell sizes are two horizontal nodes wide and one vertical node deep. Consequently, the cell volumes are not constant throughout the model. Within the focal zone, the cells cover a 4 km^2 area and are 1 km deep (Fig. 4a). Synthetic *P* and *S* traveltimes were calculated from the WEBNET earthquake locations. A vector of randomly distributed errors (±0.01 s for *P* times and ±0.02 s for *S* times) were added to the synthetic times. As with the previous synthetic tests, no synthetic cross-correlated times are used. The checkerboard WAM is calculated using the same model parameterizations as the observed data WAM. The resulting model (Fig. 4b) is well resolved within the focal zone. As expected, velocities near the surface (top 5 km) are not resolved.

A comparison of the checkerboard WAM with the WSTD values obtained from the observed data (Fig. 4c) shows that the well resolved focal zone corresponds to low experimental WSTD (WSTD $< 0.03\,\mathrm{km\,s^{-1}}$). Regions with high WSTD show smearing and poor resolution in the checkerboard WAM. The maximum WSTD is less than $0.03\,\mathrm{km\,s^{-1}}$ in the focal zone and $0.05\,\mathrm{km\,s^{-1}}$ outside of the focal zone. These maximum values are significantly lower than velocity variations observed in the focal zone. Even considering an error bar of 2σ ($\sim 95\,\%$ confidence interval), the reliability of the anomalies remains very high. Furthermore, there is no spatial correlation between the highest WSTDs and significant velocity anomalies indicating a low dependence on the initial parameters. Since the focus of the discussion is on the Vp/Vs model, the interpretation will be constrained to regions where the observed WSTD values for both the *P* and *S* model are $0.03\,\mathrm{km\,s^{-1}}$ or less.

5 Results and interpretation

In crustal rocks, compressional and shear velocities (and thus Vp/Vs) are dependent on several factors like composition, temperature, pressure, microcrack density, pore pressure and fracture density. The Vp/Vs has been used as an indicator of fluids within many earthquake settings, such as subduction zones (Husen and Kissling, 2001; Calò et al., 2012), shear zones (McLaren et al., 2008), collision zones (Scarfi et al., 2007), volcanoes (Agostinetti and Chiarabba, 2008) and hydrocarbon exploration (Zhang et al., 2009). Several studies have indicated that fluids may also play a role in the periodic swarms in Nový Kostel (Bräuer et al., 2005; Geissler et al., 2005; Hainzl et al., 2012; Špičák and Horálek 2001).

There are two main structures in the Vp/Vs WAM: the high Vp/Vs concentrated along the fault plane and the low Vp/Vs layer directly above the focal zone (Fig. 5). Within the Nový Kostel focal zone, we see a clear increase in Vp/Vs (Fig. 5). These high values are concentrated around the relocated hypocenters, which also correlates with the 169° principal fault (Vavryčuk, 2011). The base of the overlaying low Vp/Vs layer corresponds with the shallowest relocated earthquake. Above this depth (∼ 5–7 km), the Vp/Vs values are less then the regional value of 1.70 (Málek et al., 2001). These structures are interpreted in terms of local geology and the potential role of fluids in the Nový Kostel Seismic Zone.

First, we look at the average calculated values within the focal zone (Fig. 6 and Table 1). This is calculated over a lateral extent of ±4 km in x and y and 0.5 km depth intervals. As was also seen in the profiles (Fig. 5), the transition between the low Vp/Vs ratio layer and the high focal zone values occurs at 7 km depth. Within the fault zone (7–10 km depth) and overlaying layer (5–7 km depth), the mean Vp/Vs ratio is 1.73 and 1.70, respectively. The range of Vp/Vs values within the fault zone and overlaying layer are all in the documented range for igneous and metamorphic rocks, including granites and gneisses (Gercek, 2007). These ratio values are consistent with measurements of granite, gneiss and schist at 200 MPa. The higher ratios within the focal zone also correlate with phyllite measurements at 200 MPa (Christensen, 1996).

P-velocity measurements of wet and dry granitic and gneissic samples have shown that it increases with saturation (Kahraman, 2007). This has also been shown for saturated rocks under overpressured conditions (Ito et al., 1979; Popp and Kern, 1994). Even if the calculated velocity model values are dependent on the starting model, average P-velocity gradient increases with depth and a distinct decrease in average S-velocity values occurs at 7 km. The resulting high Vp/Vs ratio values observed along the fault plane may indicate that the rupture area consists of fluid-filled, fractured rock under overpressured conditions, which can be caused by fluids or their migration in the presence of a structural barrier. This is consistent with previous results showing overpressured conditions during the 1997 swarm (Vavryčuk, 2002) and the 2008 swarm (Hainzl et al., 2012). The area of high Vp/Vs values does not extend past the shallowest hypocenter indicating that any fractures and fluids are limited to the rupture zone.

Beneath the Cheb basin, the shallow and midcrust geology is dominated by the Fichtelgebirge (Smrčiny) granitic complex (Hecht et al., 1997). The geological structures underlaying the Nový Kostel Seismic Zone is known mainly from surface geology, gravity modeling (Hecht et al., 1997; Nehybka and Skácelová 1997) and the 9HR/91 high resolution refraction seismic survey (Tomek et al., 1997). Throughout the basin, the Fichtelgebirge has its base at 2–3 km, however, a large low-gravity anomaly beneath Nový Kostel indicates that the depth increases down to at least 6 km and has its root along the Mariánské-Lázně Fault (Hecht et al., 1997).

In Fig. 7, the structures observed in the Vp/Vs WAM are compared with a model derived from the 9HR/91 seismic profile and gravity modeling (Nehybka and Skácelová 1997; Tomek et al., 1997). A cross section parallel to the 9HR/91 profile but crossing through the focal zone (Fig. 7) is limited to the northwest by the station geometry. The most prominent feature in this profile is the region of low Vp/Vs directly over the focal zone (between 5 km and 7 km depth). The transition from low- to high-Vp/Vs (with respect to the regional value of 1.70) correlates with the base of the higher density metamophic unit composed of metasediments and metabasites (Nehybka and Skácelová, 1997; Weise et al., 2001). When the earthquake foci are projected onto the geological section, they concentrate within a lower density granite body. We suggest that this body may be a boundary blocking uprising magmatic fluids.

To investigate the possibility of the metamorphic unit acting as a fluid trap, we calculate the Brittleness Index (Rickman et al., 2008) for the focal zone and overlaying layer. The Brittleness Index is a relative measure of the ease with which a material fractures calculated from its Poisson Ratio and Young's modulus. A low index value indicates that a rock is resistant to fracturing and may act as a cap rock. Using a density of 2770 $\mathrm{kg\,m^{-3}}$ for the low Vp/Vs layer and 2610 $\mathrm{kg\,m^{-3}}$ for focal zone (Nehybka and Skácelová 1997; Weise et al., 2001), we find that the Brittleness Index for the overlaying layer (36.41) is indeed lower than the index for the focal zone (41.94). The lack of seismic activity within this layer confirms its lower brittleness and resistance to fracturing. As fluids are trapped below this layer, the pore pressure increases and changes the local stress field, facilitating slip along preexisting fractures or even allowing new fractures to form. Since the granite is more brittle than the metamorphic unit, the fractures probably occur there. The increased permeability allows the migration of fluid towards the surface. As the fluids migrate and the pore pressure decreases, the system returns to the initial conditions and the fluids build up again. This cycle of pore pressure increase and stress release may explain the periodic nature of the swarm seismicity in Nový Kostel.

6 Conclusions

Past studies of the Nový Kostel Seismic Zone have indicated that fluids may be an important component of the swarm cycle. This hypothesis is addressed here by analyzing the first detailed Vp/Vs model of the focal zone. The results of this study can be summarized by the following points:

- The Nový Kostel focal zone is characterized by high Vp/Vs values which concentrate along the 2008 swarm principal fault plane.
- A layer of low Vp/Vs directly overlays the fault zone.
- Earthquakes only occur below 7 km depth, which correlates with the boundary between the low and high Vp/Vs regions.
- The low Vp/Vs layer correlates to a high density metamophic unit.
- The high Vp/Vs region correlates with low density granite.
- A comparison of the Brittleness Index for the metamorphic and granite units indicates that fractures will preferentially occur in the granite. This is confirmed by the earthquake source locations.
- The low Brittleness Index of the overlaying metamorphic layer indicates that it may act as a fluid trap.

From these results, we hypothesize that the layer of low Vp/Vs acts as a trap, blocking the uprising fluids. Over time, the pore pressure increases and the granitic layer preferentially fractures due to its higher brittleness. A similar analysis of other well-documented swarms will further illuminate the structures within the Nový Kostel Seismic Zone and the role of fluids in the swarm activity.

The Supplement related to this article is available online at doi:10.5194/sed-6-511-2014-supplement.

Acknowledgements. This study was funded through the European Community's FP7 Consortium Project AIM "Advanced Industrial Microseismic Monitoring", Grant Agreement No. 230 669. We thank J. Horálek, T. Fischer, A. Boušková and the WEBNET group for providing the earthquake traveltimes and locations. V. Babuška, J. Plomerová, P. Hrubcová, W. Geissler, S. Shapiro, C. Langenbruch and an anonymous reviewer are thanked for the stimulating discussions and reviews.

References

Agostinetti, N. P. and Chiarabba, C.: Seismic structure beneath Mt Vesuvius from receiver function analysis and local earthquake tomography: evidences for location and geometry of the magma chamber, Geophys. J. Int., 175, 1298–1308, 2008.

Bankwitz, P., Schneider, G., Kämpf, H., and Bankwitz, E.: Structural characteristics of epicentral areas in Central Europe: study case Cheb Basin (Czech Republic), J. Geodyn., 35, 5–32, 2003.

Bouchaala, F., Vavryčuk, V., and Fischer, T.: Accuracy of the master-event and double-difference locations: synthetic tests and application to seismicity in West Bohemia, Czech Republic, J. Seismol., 17, 841–859, doi:10.1007/s10950-013-9357-4, 2013.

Bräuer, K., Kämpf, H., Niedermann, S., and Strauch, G.: Evidence for ascending upper mantle-derived melt beneath the Cheb basin, central Europe, Geophys. Res. Lett., 32, L08303, doi:10.1029/2004GL022205, 2005.

Calò, M., Dorbath, C., Cornet, F., and Cuenot, N.: Large-scale aseismic motion identified through 4-D P-wave tomography, Geophys. J. Int., 186, 1295–1314, doi:10.1111/j.1365-246X.2011.05108.x, 2011.

Calò, M., Dorbath, C., Luzio, D., Rotolo, S. G., and D'Anna, G.: Seismic velocity structures of southern Italy from tomographic imaging of the Ionian slab and petrological inferences, Geophys. J. Int., 191, 751–764, doi:10.1111/j.1365-246X.2012.05647.x, 2012.

Christensen, N. I.: Poisson's ratio and crustal seismology, J. Geophys. Res., 101, 3139–3156, 1996.

Fischer, T., Horálek, J., Michálek, J., and Boušková, A.: The 2008 West Bohemia earthquake swarm in the light of the WEBNET network, J. Seismol., 14, 665–682, 2010.

Geissler, W. H., Kämpf, H., Kind, R., Bräuer, K., Klinge, K., Plenefisch, T., Horálek, J., Zedník, J., and Nehybka, V.: Seismic structure and location of a CO_2 source in the upper mantle of the western Eger (Ohře) rift, central Europe, Tectonics, 24, TC5001, doi:10.1029/2004TC001672, 2005.

Gercek, G.: Poisson's ratio values for rocks, Internat. J. Rock Mechan. Mining Sci., 44, 1–13, 2007.

Hainzl, S., Fischer, T., and Dahm, T.: Seismicity-based estimation of the driving fluid pressure in the case of swarm activity in western Bohemia, Geophys. J. Int., 191, 271–281, doi:10.1111/j.1365-246X.2012.05610.x, 2012.

Hecht, L., Vigneresse, J. L., and Morteani, G.: Constraints on the origin of zonation of the granite complexes in the Fichtelgebirge (Germany and Czech Republic): evidence from a gravity and geochemical study, Geol. Rundsch., 86, S93–S109, 1997.

Heinicke, J., Fischer, T., Gaupp, R., Götze, J., Koch, U., Konietzky, H., and Stanek, S.-P.: Hydrothermal alteration as a trigger mechanism for earthquake swarms: the Vogtland/NW Bohemia region as a case study, Geophys. J. Int., 178, 1–13, doi:10.1111/j.1365-246X.2009.04138.x, 2009.

Herrmann, R. B.: FASTHYPO – a hypocenter location program, Earthquake Notes, 50, 25–37, 1979.

Hrubcová, P., Sroda, P., Špičák, A., Guterch, A., Grad, M., Keller, G. R., Brueckl, E., and Thybo, H.: Crustal and uppermost mantle structure of the Bohemian Massif based on CELEBRATION 2000 data, J. Geophys. Res., 110, B11305, doi:10.1029/2004JB003080, 2005.

Hrubcová, P., Vavryčuk, V., Boušková, A., and Horálek, J.: Moho depth determination from waveforms of microearthquakes in the West Bohemia/Vogtland swarm area, J. Geophys. Res., 118, 120–137, doi:10.1029/2012JB009360, 2013.

Husen, S. and Kissling, E.: Postseismic fluid flow after the large subduction earthquake of Antofagasta, Chili, Geology, 29, 847–850, 2001.

Ito, H., De Vilbiss, J., and Nur, A.: Compressional and shear waves in saturated rock during water-steam transition, J. Geophys. Res., 89, 4731–4735, 1979.

Kahraman, S.: The correlations between the saturated and dry P-wave velocity of rocks, Ultrasonics, 46, 341–348, 2007.

Kissling, E., Ellsworth, W. L., Eeberhart-Phillips, D., and Kradolver, U.: Initial reference models in local earthquake tomography, J. Geophys. Res., 99, 19635–19646, 1994.

Málek, J., Horálek, J., and Janský, J.: One-dimensional qP-wave velocity model of the upper crust for the West Bohemia/Vogtland earthquake swarm region, Stud. Geophys. Geod., 49, 501–524, 2001.

McLaren, M. K., Hardebeck, J. L., van der Elst, N., Unruh, J. R., Bawden, G. W., and Blair, J. L.: Complex faulting associated with the 22 December 2003 Mw 6.5 San Simeon, California, earthquake, aftershocks, and postseismic surface deformation, B. Seismol. Soc. Am., 98, 1659–1680, doi:10.1785/0120070088, 2008.

Mlčoch, B. and Skácelová, Z.: Digital elevation model of the crystalline basement of the Cheb and Sokolov Basin areas (Western Bohemia, central Europe), Z. Geol. Wissenschaft., 3, 145–152, 2009.

Nehybka, V. and Skácelová, Z.: Seismological study of the Kraslice/Vogtland-Oberpfalz region, in: Geological Model of Western Bohemia in Relation to Deep Borehole KTB in the FGR, edited by: Vrána, S. and Štrìdrá, V., J. Geol. Sci. Ser. Geol., 47, Czech Geological Survey, Prague, 186–190, 1997.

Peterek, A., Reuther, C. D., and Schunk, R.: Neotectonic evolution of the Cheb Basin (northwestern Bohemia, Czech Republic) and its implications for the late Pliocene to recent crustal deformation in the western part of the Eger Rift, Z. Geol. Wissenschaft., 39, 335–365, 2011.

Popp, T. and Kern, H.: The influence of dry and water saturated cracks on seismic velocities of crustal rocks – a comparison of experimental data with theoretical model, Surv. Geophys., 15, 443–465, 1994.

Rickman, R., Mullen, M., Petre, E., Greiser, B., and Kundert, D.: A practical use of shale petrophysics for stimulation design optimization: all shale plays are not clones of the Barnett shale, 2008 SPE Annual Technical Conference and Exhibition, Denver, Colorado, USA, 21–24 September 2008, SPE 115258, 2008.

Růžek, B., Hrubcová, P., Novotný, M., Špičák, A., and Karousová, O.: Inversion of travel times obtained during active seismic refraction experiments CELEBRATION 2000, ALP 2002 and SUDETES 2003, Stud. Geophys. Geod., 51, 141–164, 2007.

Scarfì, L., Giampiccolo, E., Musumeci, C., Patanè, D., and Zhang, H.: New insights on 3D crustal structure in southeastern Sicily (Italy) and tectonic implications from an adaptive mesh seismic tomography, Phys. Earth Planet. In., 161, 74–85, 2007.

Špičák, A. and Horálek, J.: Possible role of fluids in the process of earthquake swarm generation in the West Bohemia/Vogtland seismoactive region, Tectonophysics, 336, 151–161, 2001.

Švancara, J., Havíř, J., and Conrad, W.: Derived gravity field of the seismogenic upper crust of SE Germany and West Bohemia and its comparison with seismicity, Stud. Geophys. Geod., 52, 567–588, 2008.

Tomek, È., Dvořáková, V., and Vrána, S.: Geological interpretation of the 9HR and 503M seismic profiles in Western Bohemia, edited by: Vrána, S. and Štrědrá, V., J. Geol. Sci. Ser. Geol., 47, Czech Geological Survey, Prague, 43–50, 1997.

Vavryčuk, V.: Non-double-couple earthquakes of January 1997 in West Bohemia, Czech Republic: evidence of tensile faulting, Geophys. J. Int., 149, 364–373, doi:10.1046/j.1365-246X.2002.01654.x, 2002.

Vavryčuk, V.: Principal earthquakes: theory and observations for the 2008 West Bohemia swarm, Earth Planet. Sc. Lett., 305, 290–296, doi:10.1016/j.epsl.2011.03.002, 2011.

Waldhauser, F. and Ellsworth, W. L.: A double-difference earthquake location algorithm: method and application to the Hayward fault, B. Seismol. Soc. Am., 90, 1353–1368, 2000.

Weise, S. M., Bräuer, K., Kämpf, H., Strauch, G., and Koch, U.: Transport of mantle volatiles through the crust traced by seismically released fluids: a natural experiment in the earthquake swarm area Vogtland/NW Bohemia, Central Europe, Tectonophysics, 336, 137–150, 2001.

Zhang, H. and Thurber, C. H.: Double-difference tomography: the method and its application to the Hayward fault, California, B. Seismol. Soc. Am., 93, 1175–1189, 2003.

Zhang, H., Sarkar, S. Toksöz, M. N., Kueli, H. S., and Al-Kindy, F.: Passive seismic tomography using induced seismicity at a petroleum field in Oman, Geophysics, 74, WCB57–WCB69, doi:10.1190/1.3253059, 2009.

Table 1. Average velocities within the Nový Kostel focal zone.

Depth (km)	Mean P-Velocity ($\mathrm{km\,s^{-1}}$)	Mean S-Velocity ($\mathrm{km\,s^{-1}}$)	Mean Vp/Vs Ratio
5	6.10	3.58	1.70
5.5	6.19	3.64	1.70
6	6.28	3.71	1.69
6.5	6.37	3.76	1.69
7	6.46	3.80	1.70
7.5	6.55	3.83	1.71
8	6.62	3.84	1.73
8.5	6.69	3.85	1.74
9	6.77	3.87	1.75
9.5	6.86	3.90	1.76
10	6.94	3.94	1.76

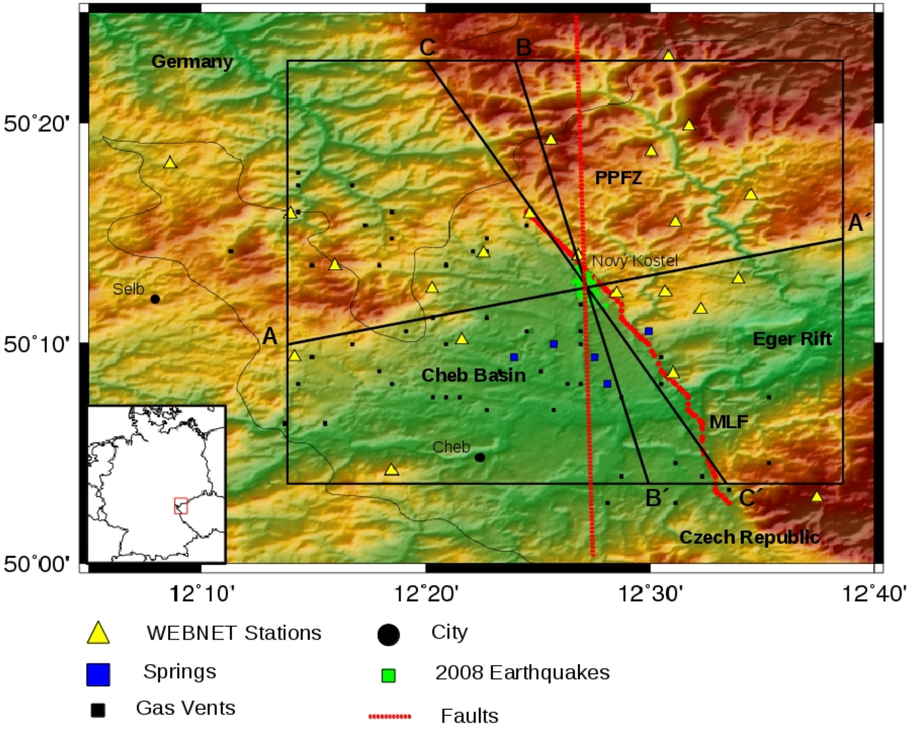

Figure 1. Topographic map showing the Nový Kostel seismic zone. Abbreviations: MLF – Mariánské-Lázně Fault, PPFZ – Počátky-Plesná Fault Zone. Mineral spring and gas vent locations digitized from Heinike et al. (2009).

Title Page
Abstract Introduction
Conclusions References
Tables Figures
◄ ►
Back Close
Full Screen / Esc
Printer-friendly Version
Interactive Discussion

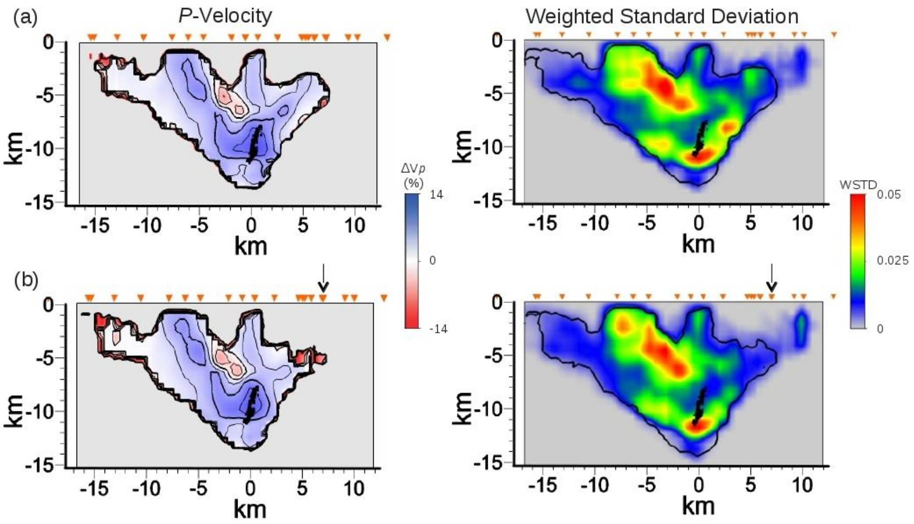

Figure 2. *P*-velocity Weighted Average Model (WAM) and Weighted Standard Deviation (WSTD) for **(a)** all stations and **(b)** selected stations. Arrow indicates station removed from the dataset. Only areas constrained by the data are shown. *P*-velocities are shown as percent difference from the regional model of Málek et al. (2001).

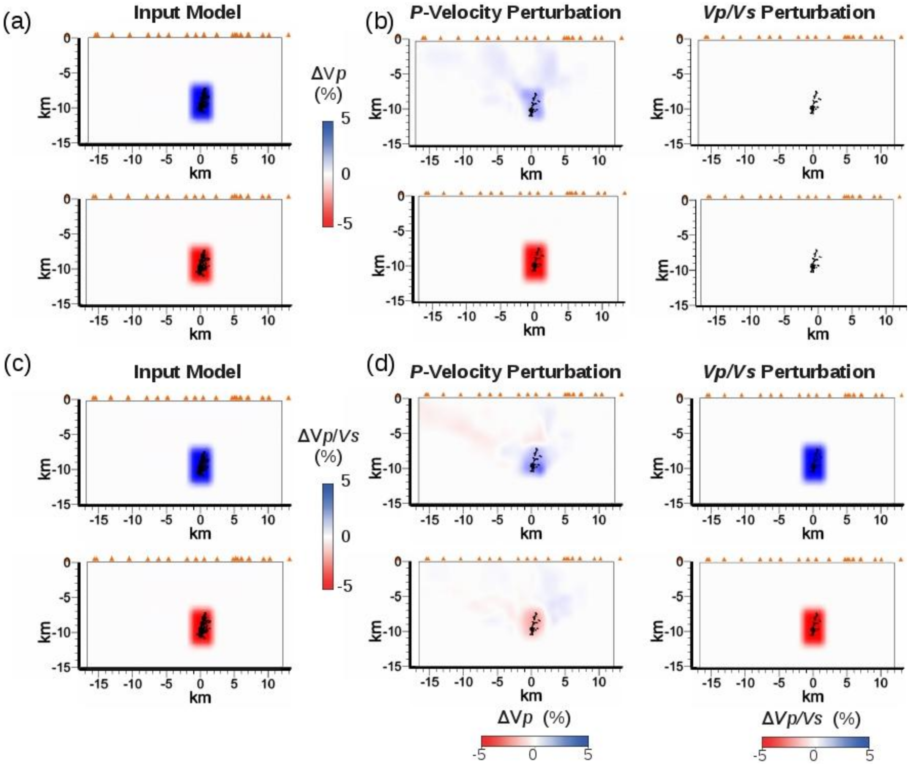

Figure 3. Anomaly restoration synthetic test. A block 3 km wide in the *x*-direction, 6 km wide in the *y*-direction, 5 km deep and enclosing all earthquakes is perturbed. Within the block, **(a)** *P*-velocities are modified by ±5 % or **(c)** Vp/Vs ratio is perturbed by ±5 %. All velocities and ratios outside the block correspond to the regional model of Málek et al. (2001). The recovered models (**b** and **d**) all show that the Vp/Vs is well recovered. The recovered *P*-velocity models show some smearing and are also influenced by fluctuation in the Vp/Vs ratio.

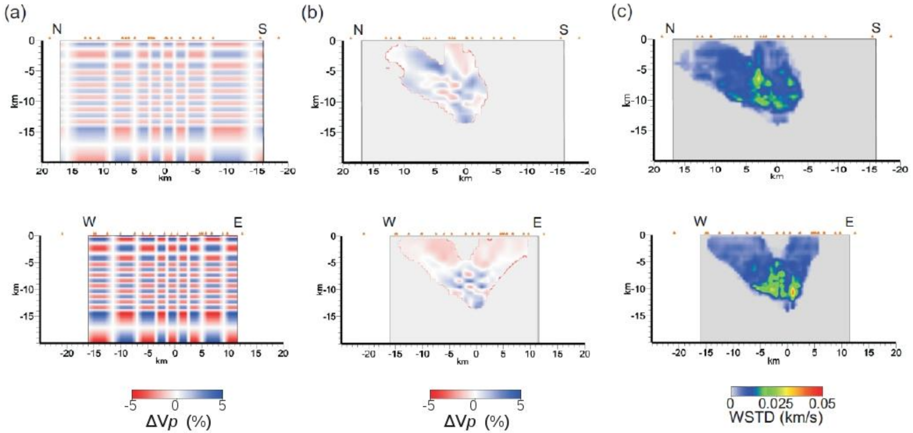

Figure 4. Checkerboard resolution test. North–south and east–west profiles showing **(a)** the starting checkerboard model with a 5 % variation in *P*-velocity, **(b)** the recovered Weighted Average Model (WAM) and **(c)** the Weighted Standard Deviation (WSTD) from the observed data. Shallow areas (depth less than 5 km) are not resolved. Within the focal zone, areas with poor checkerboard resolution coincide with WSTD values greater than 0.03 km s^{-1}. Only areas constrained by the data are shown.

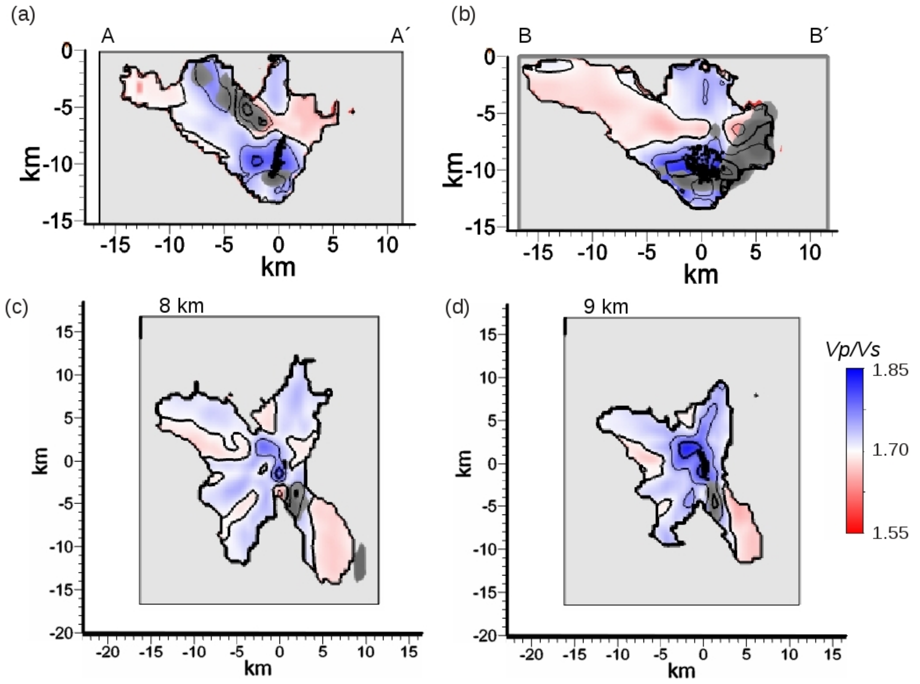

Figure 5. Vp/Vs ratio Weighted Average Model. In the across-strike **(a)** and along-strike **(b)** profiles, the focal zone is characterized by high Vp/Vs values. Depth slices through the hypocenters at 8 km **(c)** and 9 km **(d)** show that these higher values concentrate along the fault plane (**c** and **d**). An almost-continuous layer of low Vp/Vs overlays the hypocenters between 5 km and 7 km. Grey mask shows areas with WSTD greater than 0.03 km s^{-1}. Only areas constrained by the data are shown. Earthquake hypocenters are projected onto the profiles and depth slices.

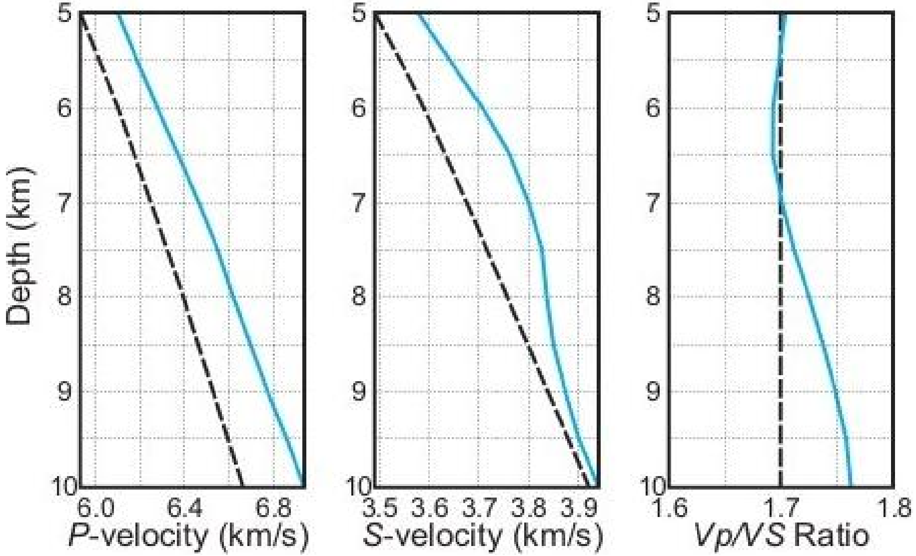

Figure 6. Average velocities and Vp/Vs ratio values within the focal zone. The average WAM values (solid lines) are calculated for all resolved nodes within ±4 km from the grid origin and in 1 km thick layers. Dashed lines indicate the regional model from Málek et al. (2001).

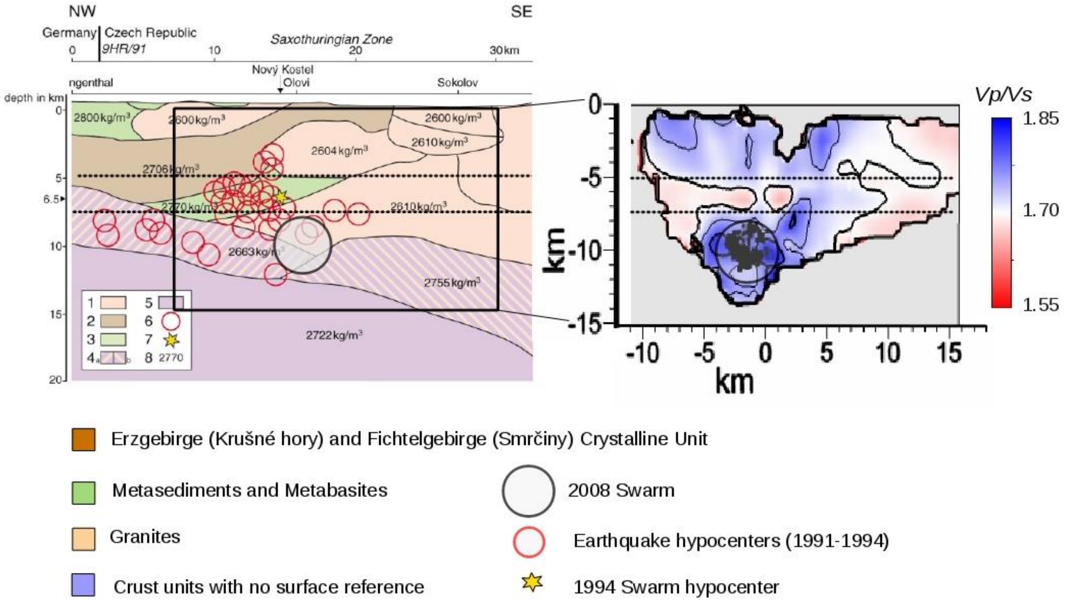

Figure 7. Comparison between Vp/Vs Weighted Average Model (right) and a geological interpretation (left) based on the 9HR/91 seismic profile and gravity modeling (Nehybka and Skácelová 1997; Tomek et al., 1997). The Vp/Vs model profile is parallel to 9HR/91 and through the focal zone. Dashed lines show the low Vp/Vs layer and the black circle shows the 2008 swarm. Only areas constrained by the data are shown. Geological profile (left) after Weise et al. (2001).